



# CHORUS

This is the accepted manuscript made available via CHORUS. The article has been published as:

## Equivalence principle violation in weakly Vainshtein-screened systems

Alexander V. Belikov and Wayne Hu

Phys. Rev. D **87**, 084042 — Published 17 April 2013

DOI: [10.1103/PhysRevD.87.084042](https://doi.org/10.1103/PhysRevD.87.084042)

# Equivalence Principle Violation in Weakly Vainshtein-Screened Systems

Alexander V. Belikov<sup>1</sup> and Wayne Hu<sup>2</sup>

<sup>1</sup>*Institut d'Astrophysique de Paris, UMR 7095 CNRS,*

*Université Pierre et Marie Curie, 98 bis Boulevard Arago, Paris 75014, France*

<sup>2</sup>*Kavli Institute for Cosmological Physics, Department of Astronomy & Astrophysics,  
Enrico Fermi Institute, University of Chicago, Chicago, IL 60637*

Massive gravity, galileon and braneworld models that modify gravity to explain cosmic acceleration utilize the nonlinear field interactions of the Vainshtein mechanism to screen fifth forces in high density regimes. These source-dependent interactions cause apparent equivalence principle violations. In the weakly-screened regime violations can be especially prominent since the fifth forces are at near full strength. Since they can also be calculated perturbatively, we derive analytic solutions for the cubic galileon: the motion of massive objects in compensated shells and voids and infall toward halos that are spherically symmetric. Using numerical techniques we show that these solutions are valid until the characteristic scale becomes comparable to the Vainshtein radius. We find a relative acceleration of more massive objects toward the center of a void and a reduction of the infall acceleration that increases with the mass ratio of the halos which can in principle be used to test the Vainshtein screening mechanism.

## I. INTRODUCTION

In models that seek to explain the current acceleration of the cosmic expansion by modifications to gravity or the addition of universal fifth forces on cosmological scales, such modifications must be hidden from local tests by so-called screening mechanisms. Screening mechanisms invoke nonlinearity in the equations of motion for the field that mediates the extra force.

The Vainshtein screening mechanism [1, 2] was first introduced in the context of massive gravity to suppress the propagation of additional helicity modes [3, 4]. Here nonlinear derivative interactions of the field act to screen the fifth force within the so-called Vainshtein radius around a matter source. The Vainshtein mechanism occurs not only in modern incarnations of Boulware-Deser [5] ghost-free massive gravity [6–9] but also in galileon cosmology [10–16] and braneworld models [17–23]. For definiteness, we take the DGP braneworld model [27] which exhibits the cubic galileon interaction.

In these models, all bodies accelerate equivalently in the total field of the fifth force and hence obey a microscopic equivalence principle. Nonetheless screened bodies do not move as test bodies in an external field leading to an apparent or macroscopic violation of the equivalence principle [24]. Instead, nonlinearity in the field interactions causes interference between the external and body field in forming the total field [25]. In the Vainshtein mechanism, this interference occurs when the second spatial derivatives of the fields becomes large enough that the self-interaction terms become important, i.e. within the Vainshtein radius of the external and body sources.

A general technique was recently introduced for determining such effects in two-body systems by considering the effective density generated by the nonlinear interaction [26]. It was applied to the Earth-Moon system, which exhibits strong screening since the orbit of the Moon is well within the Vainshtein radius of both the Earth and the Moon. Violations of the equivalence prin-

ciple thus appear as a small mass-dependent correction on the already suppressed effect of anomalous perihelion precession. Here we study the weakly-screened limit where the Vainshtein mechanism is only beginning to operate. These cases have the advantage that fifth forces are only weakly suppressed and that equivalence principle violations are analytically solvable by a perturbative expansion. Weak screening is applicable to cosmological situations such as voids and the outskirts of dark matter halos.

The outline of this paper is as follows. We begin in §II with a review of the Vainshtein mechanism and develop the effective density approach for the weak-screening regime. In §III, we consider several examples where the acceleration of massive bodies can be analytically calculated. In §IV, we test the limits of validity for the weak-screening approximation. We discuss these results in §V.

## II. WEAK SCREENING

For models that exhibit Vainshtein screening, the ordinary Newtonian potential is modified by the addition of a scalar field  $\phi$  which itself obeys a nonlinear Poisson equation

$$3\beta\nabla^2\phi + N[\phi, \phi] = 8\pi G\delta\rho, \quad (1)$$

where  $\beta$  is a parameter that determines the coupling to matter density fluctuations from the cosmological mean  $\delta\rho = \rho - \bar{\rho}$ . For definiteness, we take the Dvali-Gabadadze-Porrati (DGP) braneworld example [27] where the derivative operator is given by

$$N[\phi_1, \phi_2] = r_c^2 [\nabla^2\phi_1\nabla^2\phi_2 - \nabla_i\nabla_j\phi_1\nabla^i\nabla^j\phi_2] \quad (2)$$

in the quasistatic approximation. Here  $r_c$  is the crossover scale and determines the strength of the nonlinear interactions. We have written out this derivative interaction

term in a general bilinear form to facilitate its use in two-body systems [26].

For a single, spherically symmetric body of mass  $M$  it is straightforward to show that fifth forces are screened within the Vainshtein scale (e.g. [23])

$$r_{*M} = \left( \frac{16GMr_c^2}{9\beta^2} \right)^{1/3}. \quad (3)$$

For example, we can define a weak-screening regime exterior to this scale where [26]

$$\phi_M \approx -\frac{2GM}{3\beta r} \left( 1 - \frac{1}{16} \frac{r_{*M}^3}{r^3} \right), \quad r \gg r_{*M}. \quad (4)$$

For two bodies, there is an additional screening that can be expressed as the interference between the fields of the individual bodies. Given two sources  $\delta\rho_M$  and  $\delta\rho_m$ , which individually produce fields  $\phi_M$  and  $\phi_m$  satisfying

$$3\beta\nabla^2\phi_{M,m} + N[\phi_{M,m}, \phi_{M,m}] = 8\pi G\delta\rho_{M,m}, \quad (5)$$

jointly  $\phi_M + \phi_m$  no longer solves Eq. (1) for  $\delta\rho_M + \delta\rho_m$ . Instead, the interference field [26]

$$\phi_\Delta \equiv \phi - \phi_M - \phi_m, \quad (6)$$

solves Eq. (1) if

$$3\beta\nabla^2\phi_\Delta = -2N[\phi_M, \phi_m] - 2N[\phi_M + \phi_m, \phi_\Delta] - N[\phi_\Delta, \phi_\Delta]. \quad (7)$$

Thus the real density fields  $\delta\rho_M$  and  $\delta\rho_m$  are eliminated in favor of an effective density field given by the nonlinear interaction terms. Note that the real density fields can themselves be composite systems of  $n$  individual bodies so long as the solutions  $\phi_M$  and  $\phi_m$  are known. In general this system remains a nonlinear Poisson equation, amenable only to numerical techniques [21, 28, 29].

Now let us consider the weak-screening limit. By taking  $r_c^2 \rightarrow 0$ , we can iteratively solve for joint screening effects order-by-order in  $r_c^2$ . To leading order  $\phi_\Delta = \mathcal{O}(r_c^2)$  and Eq. (7) can be approximated as

$$3\beta\nabla^2\phi_\Delta^{(0)} = -2N[\phi_M, \phi_m], \quad (8)$$

which is now a linear Poisson equation with an external effective density. Using this leading order expression, we can find the first order correction by solving

$$3\beta\nabla^2\phi_\Delta^{(1)} = -2N[\phi_M + \phi_m, \phi_\Delta^{(0)}], \quad (9)$$

etc. Convergence of this series checks the validity of the approximation. By dimensional analysis, the series should converge so long as  $r_{*M}/s \ll 1$  and  $r_{*m}/s \ll 1$  where  $s$  is the typical physical scale of the system, e.g. the separation between bodies (see §IV).

The weak-screening limit for two-body interactions can apply even if near the individual bodies the individual fields enter a strong-screening regime. For example near

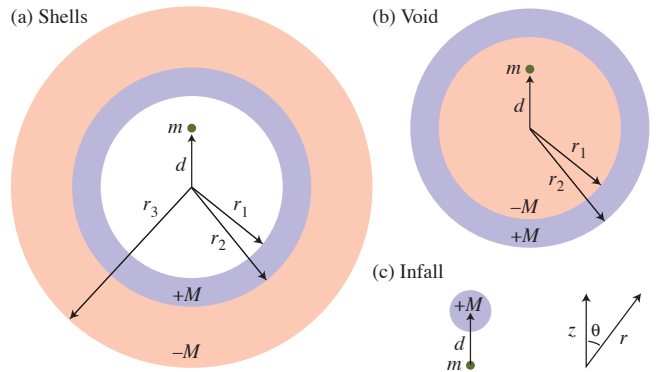


FIG. 1. Weak screening examples: (a) compensated shells with  $\delta\rho_M = 0$  in the interior and mass  $\pm M$  in the shells; (b) compensated void with an underdensity of mass  $-M$  in the center and  $+M$  in the shell; (c) infall toward onto a spherical mass  $M$ . The smaller point particle, whose motion we study, is labeled  $m$ .

the location of mass  $m$ ,  $\phi_m$  may actually be strongly self-screened if the physical size of the body is smaller than its Vainshtein radius. All that is required for two-body weak screening is that the interference source  $N$  is dominated by the weakly-screened far-fields and that it generates an interference field  $\phi_\Delta$  that is nearly a pure gradient across the Vainshtein radius of  $m$  [24]. Higher order contributions from Eq. (8) are therefore small since the second derivatives of  $\phi_\Delta$  are small where those of  $\phi_m$  are large.

### III. ANALYTIC EXAMPLES

In this section, we consider three examples of equivalence principle violation in weakly-screened systems where the mass-dependent acceleration of bodies in the system can be solved analytically: empty, compensated mass shells; negative density fluctuation, compensated voids; and infall into a spherically symmetric body.

#### A. Shells

In Newtonian mechanics the shell theorem says that a body inside a spherically symmetric shell does not experience a force from the shell. Despite the lack of a purely  $1/r^2$  force under the Vainshtein mechanism (see e.g. Eq. 4), it remains true that a test body of infinitesimal mass inside the shell does not experience a force (see e.g. [23]). However for a finite mass  $m$ , the nonlinear interaction between the body field and shell field causes a force unless the body is at the center of the shell. This effect is common to gravitational field equations that are nonlinear. In general relativity its impact is suppressed by the strength of the nonlinearity, i.e. the ratio of the Schwarzschild radius of the body to the separation  $Gm/s$ ,

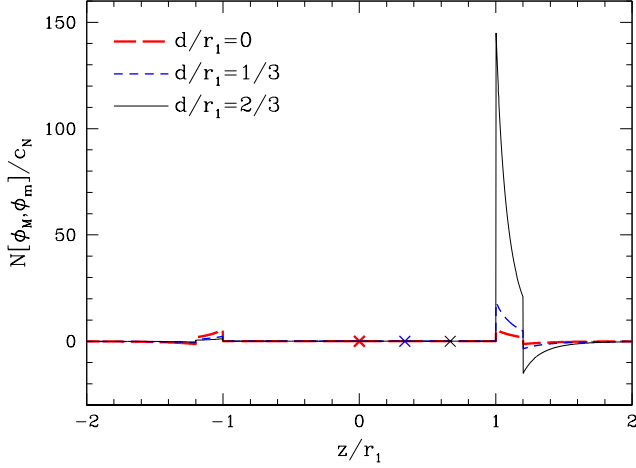


FIG. 2. Effective density as a function of  $z = r \cos \theta$  for the shells case of Fig. 1a with  $r_2 = 1.2r_1$  and  $r_3 \rightarrow \infty$  and several choices of the displacement  $d$  of the particle from the center of the shell (crosses). As the particle is displaced further along the  $+z$  axis, the effective density in the shells exhibits an increasing asymmetry which leads to the net force.

and in Modified Newtonian Dynamics it appears unsuppressed in the deeply nonlinear regime [30].

To set up this first test case, we take  $\delta\rho_M$  to contain a constant-density shell that encloses a mass of  $+M$  between  $r_1 < r \leq r_2$ . In order to ensure compatibility with cosmological boundary conditions where the mean density fluctuation is zero, we take an additional outer shell of  $-M$  between  $r_2 < r \leq r_3$ . Note that in the limit  $r_3 \rightarrow \infty$  the result will be the same as an uncompensated single shell. We obtain the  $\phi_M$  solution to zeroth order in  $r_c^2$  by superimposing the Newtonian solutions for a tophat constant density enclosing a mass  $M_{\text{th}}$  within the radius  $r_{\text{th}}$

$$\phi_{\text{th}} = -\frac{2}{3\beta} \frac{GM_{\text{th}}}{r_{\text{th}}} \begin{cases} \left(\frac{3}{2} - \frac{r^2}{2r_{\text{th}}^2}\right) & r \leq r_{\text{th}} \\ \frac{r_{\text{th}}}{r} & r > r_{\text{th}} \end{cases}. \quad (10)$$

Superimposing tophats of the appropriate mass,  $\phi_M = \text{const.}$  for  $r \leq r_1$  and 0 for  $r > r_3$ .

Next we take a small body of mass  $m$  displaced along the  $z$  axis at  $z = d < r_1$  so as to be inside the shell (see Fig. 1a). It suffices to consider this mass to be uncompensated. If we place a compensating shell of  $-m$  at  $r > r_3$ , we obtain identical results since there can be no interference with the  $\phi_M = 0$  field there. More specifically,  $N[\phi_M, \phi_m]$  has compact support and is only non-vanishing for  $r_1 < r \leq r_3$

$$N[\phi_M, \phi_m] = c_N r_1^6 F(r, \theta) \begin{cases} \frac{r_1^3}{r_2^3 - r_1^3} & r_1 < r \leq r_2 \\ \frac{r_3^3}{r_2^3 - r_3^3} & r_2 < r \leq r_3 \\ 0 & \text{else} \end{cases} \quad (11)$$

with

$$F(r, \theta) = \frac{d^2 + 4r^2 - 8dr \cos \theta + 3d^2 \cos(2\theta)}{r^3(d^2 + r^2 - 2dr \cos \theta)^{5/2}} \quad (12)$$

and

$$c_N = \frac{2r_c^2 G^2 M m}{3\beta^2 r_1^6} = \frac{3}{8} \frac{GM}{r_1^3} \left(\frac{r_{*m}}{r_1}\right)^3, \quad (13)$$

where  $r_{*m}$  is the Vainshtein radius of  $m$  in isolation.

Even if  $\phi_m$  were in the deep screening regime near the location of  $m$ , there would still be no effective density there since  $\phi_M$  is constant inside the shell. Thus we can safely take the limit of a point mass particle. In Fig. 2, we show how the effective density changes as the point mass is taken from the center of the shell toward the edge. Note the asymmetry that develops between the near and far side of the shell.

We can build our solution for  $\phi_\Delta$  from that of the following electrostatics-like Poisson equation

$$\nabla^2 \Phi = \begin{cases} 0 & r \leq r_0 \\ -F(r, \theta) & r_0 < r < \infty \end{cases}. \quad (14)$$

More specifically, we are interested in calculating the potential gradient  $\nabla \Phi = \partial \Phi / \partial z$  at a position of the particle  $r = d$  and  $\theta = 0$ , or the “electric field” at that point

$$\begin{aligned} \frac{\partial \Phi}{\partial z} &= \frac{1}{2} \int_{r_0}^{\infty} r^2 dr \int_0^\pi \sin \theta d\theta \frac{(r \cos \theta - d)F(r, \theta)}{(r^2 + d^2 - 2rd \cos \theta)^{3/2}} \\ &= \frac{1}{d^5} I(r_0/d), \end{aligned} \quad (15)$$

where

$$I(x) = \frac{x^2 + 1}{4x^2(x^2 - 1)^2} + \frac{1}{8x^3} \ln \left( \frac{x - 1}{x + 1} \right). \quad (16)$$

In the  $d \rightarrow 0$  limit,  $x \rightarrow \infty$  and  $I(x) \approx 2/(3x^6)$ .

We again superimpose these solutions with the appropriate  $r_0$  to construct the full solution

$$\begin{aligned} \frac{\partial \phi_\Delta}{\partial z} \Big|_m &= c_g \left(\frac{r_1}{d}\right)^5 \left\{ \frac{r_1^3}{r_2^3 - r_1^3} [I(r_1/d) - I(r_2/d)] \right. \\ &\quad \left. - \frac{r_3^3}{r_3^3 - r_2^3} [I(r_2/d) - I(r_3/d)] \right\}, \end{aligned} \quad (17)$$

where

$$c_g = \frac{4r_c^2 G^2 M m}{9\beta^3 r_1^5} = \frac{1}{4\beta} \frac{GM}{r_1^2} \left(\frac{r_{*m}}{r_1}\right)^3. \quad (18)$$

Note that  $c_g$  scales as the shell acceleration  $GM/\beta r_1^2$  suppressed by the cube of the Vainshtein scale over the characteristic distance. That  $\partial \phi_\Delta / \partial z \propto Mm$  is a consequence of the bilinearity of the effective density.

Examples of the acceleration as a function of  $d/r_1$  are shown in Fig. 3. One interesting limit is an infinitesimally thin shell  $r_2 \rightarrow r_1$  with vanishing impact from cosmological compensation  $r_3 \rightarrow \infty$

$$\frac{\partial \phi_\Delta}{\partial z} \Big|_m = c_g \left[ \frac{2}{3} \frac{d/r_1}{(1 - d^2/r_1^2)^3} \right]. \quad (19)$$

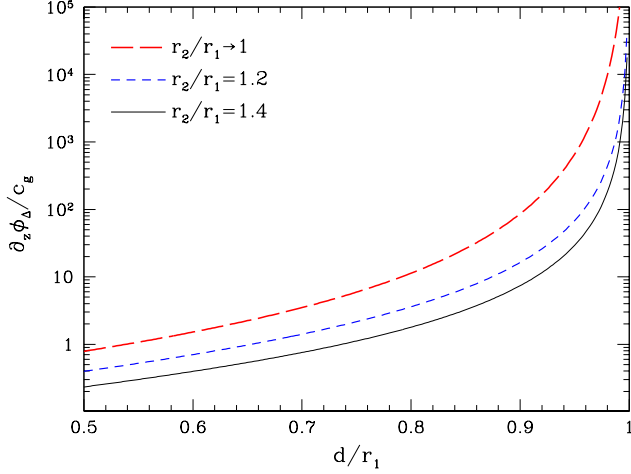


FIG. 3. Acceleration or field gradient as a function of distance  $d/r_1$  from center for various shell widths given by  $r_2/r_1$  and  $r_3 \rightarrow \infty$ . As the particle approaches the shell, the acceleration increases as  $s^{-3}$ , where  $s = r_1 - d$ , with a proportionality constant that reaches a maximum as the shell width goes to zero  $r_2/r_1 \rightarrow 1$ .

Consider the cases where the particle is near the center or near the shell. For the former case, there is a suppression of  $(r_{*m}/r_1)^3(d/r_1)$  from the scale of the Newtonian acceleration of the shell mass. The first factor accounts for the weak nonlinearity of the system. The second factor accounts for the fact that by symmetry the force must vanish if  $d = 0$ .

In the opposite regime where the particle is closer to the shell than the center, the acceleration scales strongly with distance to shell  $s = r_1 - d$ . In particular as the particle approaches the shell

$$\lim_{s \rightarrow 0} \frac{\partial \phi_\Delta}{\partial z} \Big|_m = \frac{1}{6\beta} \frac{GM}{r_1^2} \left( \frac{r_{*m}}{2s} \right)^3, \quad (20)$$

such that there is a suppression factor of the Vainshtein radius compared to the distance to the shell (see Fig. 3).

In this case, we see the impact of the nonlinearity of the field equations unobscured by symmetry. Once the Vainshtein screened regime of  $m$  starts to overlap the shell, the field of the shell effectively creates a boundary condition there, much like the establishment of a mirror charge by a conductor. Since the Vainshtein radius of the particle depends on its mass, the equivalence principle is macroscopically broken: for an attractive fifth force, the acceleration of a particle towards the center will grow linearly with the mass  $m$ . The sign of the effect is determined by the fact that the Vainshtein correction in Eq. (4) makes the force fall away with distance less rapidly than  $1/r^2$  and so the far side of the shell that contributes more force than the near side.

## B. Void

A closely related and more observationally relevant case is a cosmological void. In this case instead of an interior at the mean cosmological density and  $\delta\rho_M = 0$ , we have an underdensity. We can idealize the void as a spherical tophat of spatially constant underdensity  $\delta\rho_M = \bar{\rho}\Delta_V$  where  $-1 \leq \Delta_V < 0$  for  $r \leq r_1$  with a total negative mass fluctuation of

$$-M = \frac{4\pi}{3} r_1^3 \bar{\rho} \Delta_V. \quad (21)$$

The void is surrounded by a positive density shell of mass  $+M$  for  $r_1 < r \leq r_2$  such that the total mass fluctuation exterior to  $r_2$  is zero (see Fig. 1b). The Vainshtein scale of such a void is

$$r_{*M} = r_1 \left( \frac{8\Omega_m H_0^2 r_c^2}{9\beta^2} |\Delta_V| \right)^{1/3} \quad (22)$$

and so for  $H_0 r_c / \beta \lesssim 1$ , a void of any size  $r_1$  is in the weak-screening regime throughout its interior.

Despite the fact that the interior now has a finite  $\delta\rho_M$ , the void and shell case are nearly identical. The reason is that if  $\phi_M$  is the  $r^2$ -field associated with a constant density source, then

$$N[\phi_M, \phi_m] = \frac{2}{3} r_c^2 \nabla^2 \phi_M \nabla^2 \phi_m \quad (23)$$

regardless of the form of  $\phi_m$  [26].

For a particle of mass  $m$ , the effective density therefore vanishes inside the void except at the position of the test mass. If we take the particle to be a constant density spherical tophat with  $\rho_m$  that vanishes outside its radius  $r_m \ll r_1$

$$N[\phi_M, \phi_m] = \frac{2r_c^2 G^2}{3\beta^2} \begin{cases} \left(\frac{8\pi}{3}\right)^2 \bar{\rho} \Delta_V \rho_m & r \leq r_1 \\ \frac{r^3}{r_2^3 - r_1^3} M m F(r, \theta) & r_1 < r \leq r_2 \\ 0 & r > r_2 \end{cases} \quad (24)$$

The  $r \leq r_1$  term provides no acceleration at the position of the test mass by symmetry and the shell term gives

$$\frac{\partial \phi_\Delta}{\partial z} \Big|_m = c_g \left( \frac{r_1}{d} \right)^5 \frac{r_2^3}{r_2^3 - r_1^3} \left[ I\left(\frac{r_1}{d}\right) - I\left(\frac{r_2}{d}\right) \right], \quad (25)$$

which has a form very similar to Eq. (17). In particular the infinitesimal width  $r_2 \rightarrow r_1$  case has the limiting behaviors

$$\begin{aligned} \lim_{d/r_1 \rightarrow 0} \frac{\partial \phi_\Delta}{\partial z} \Big|_m &= \frac{1}{3\beta} \frac{GM}{r_1^2} \left( \frac{r_{*m}}{r_1} \right)^3 \frac{d}{r_1}, \\ \lim_{s/r_1 \rightarrow 0} \frac{\partial \phi_\Delta}{\partial z} \Big|_m &= \frac{1}{6\beta} \frac{GM}{r_1^2} \left( \frac{r_{*m}}{r_1} \right)^3 \left( \frac{r_{*m}}{2s} \right)^3, \end{aligned} \quad (26)$$

where recall  $s = r_1 - d$  is the separation between the particle and the shell. In the later limit, the shell and void cases are identical as one might expect.

Halos in compensated spherical voids therefore accelerate differently depending on their mass when they are near a Vainshtein radius  $r_{*m}$  of the shell. The Vainshtein radius of a halo scales with its virial radius. Taking the virial radius of the halo  $r_H$  as the radius out to which the average interior density reaches  $\Delta_H \sim 200$ , we obtain the Vainshtein radius of a halo of mass  $m$

$$r_{*m} = r_H \left( \frac{8\Omega_m H_0^2 r_c^2}{9\beta^2} |\Delta_H| \right)^{1/3}. \quad (27)$$

For  $H_0 r_c / \beta \lesssim 1$ , halos that are near a virial radius of the compensating shell will be accelerated away from the shell.

### C. Infall

Lastly we consider the problem of two point masses, or tophat constant density bodies of radius negligible compared with their separation. This problem was solved numerically in the strong-screening regime in Ref. [26]. Here we consider the weak-screening regime as might be appropriate for a satellite dark matter halo of mass  $m$  falling through the virial radius of a parent halo of mass  $M$ .

In this case, each mass in isolation carries a field given by Eq. (4), e.g.

$$\phi_m \approx -\frac{2Gm}{3\beta R}, \quad (28)$$

for the satellite mass and likewise for the parent mass  $M$ . For convenience, we place  $M$  at  $(r = 0, z = d)$  and  $m$  at the origin  $(r = 0, z = 0)$  (see Fig. 1c). The effective density becomes

$$N[\phi_M, \phi_m] = -\frac{2}{3} \frac{r_c^2}{\beta^2} G^2 M m F(r, \theta). \quad (29)$$

The main difference between this case and the previous cases is that the effective density does not have compact support and indeed diverges at the position of the two bodies.

Nonetheless, just like for the divergent physical densities of point masses, we can still evaluate the forces induced by one body on the other. At the position of the satellite mass  $m$

$$\begin{aligned} \left. \frac{\partial \phi_\Delta}{\partial z} \right|_m &= -\frac{2}{9} \frac{r_c^2}{\beta^3} G^2 M m \int_0^\infty r^2 dr \int_0^\pi \sin \theta d\theta F(r, \theta) \frac{\cos \theta}{r^2} \\ &= \frac{8}{27} \frac{r_c^2}{\beta^3} \frac{G^2 M m}{d^5} = \frac{1}{6\beta} \frac{GM r_{*m}^3}{d^5}. \end{aligned} \quad (30)$$

Since  $\phi_m$  is symmetric around the origin, it provides no acceleration there and the total is

$$\left[ \frac{\partial \phi_M}{\partial z} + \frac{\partial \phi_\Delta}{\partial z} \right]_m = -\frac{2GM}{3\beta d^2} \left( 1 - \frac{r_{*M}^3 + r_{*m}^3}{4d^3} \right) \quad (31)$$

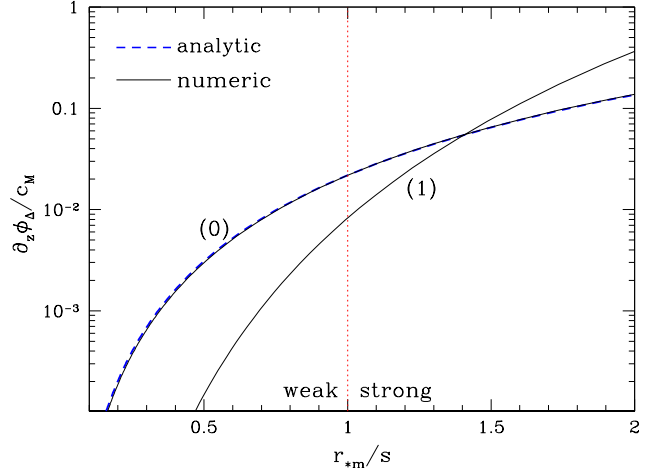


FIG. 4. Numerical test of weak screening. Numerical results for the leading order acceleration “(0)” in the weak-screening approximation agree well with the analytic expression from Eq. (17) while those for the first order correction “(1)” from Eq. (9) indicate that the approximation is valid until the distance to the shell  $s$  is smaller than a Vainshtein radius of the body  $r_{*m}$  (vertical dashed line). These terms have opposite sign, implying that the acceleration ceases to grow as rapidly in the strong screening regime. See text for the shell parameters of this example.

such that the acceleration of  $m$  from the field of  $M$  is reduced by  $(r_{*M}^3 + r_{*m}^3)/d^3$ . Note that we have kept here the  $\mathcal{O}(r_c^2)$  correction to  $\phi_A$  from Eq. (4) to maintain the same order in  $r_c$  throughout. The impact of the two-body interference for  $m \ll M$  is thus muted by the fact that the main suppression still comes from the screening of the larger mass. As the two masses become comparable, the interference can make a more substantial reduction of the attractive force.

This calculation also illustrates the role of the effective density in restoring momentum conservation or Newton’s third law. By symmetry, this calculation also gives the acceleration of body  $M$  from the field of  $m$

$$\left[ \frac{\partial \phi_m}{\partial z} + \frac{\partial \phi_\Delta}{\partial z} \right]_M = \frac{2Gm}{3\beta d^2} \left( 1 - \frac{r_{*m}^3 + r_{*M}^3}{4d^3} \right). \quad (32)$$

The sum of the two forces

$$m \left[ \frac{\partial \phi_M}{\partial z} + \frac{\partial \phi_\Delta}{\partial z} \right]_m + M \left[ \frac{\partial \phi_m}{\partial z} + \frac{\partial \phi_\Delta}{\partial z} \right]_M = 0, \quad (33)$$

whereas without the interference the balance would be grossly violated for  $m/M \ll 1$  [26].

## IV. BEYOND WEAK SCREENING

We expect the weak-screening regime to extend to the point at which the Vainshtein radii of the individual bodies is comparable to the characteristic distances in the

system. In our perturbative approach, the breakdown of weak screening is monitored by the next to leading order term  $\phi_{\Delta}^{(1)}$  in Eq. (9). In this section we shall check to see when this breakdown occurs numerically.

For illustration purposes, we choose the shell test case (see Fig. 1). Given that the effective density  $N$  vanishes for  $r > r_3$ , this case has periodic boundary conditions and can be solved efficiently with fast Fourier transform techniques.

As an example, we take the outer shell to be inscribed inside the cube of side length  $L = 1024$  pixels:  $r_3 = L/2$ . We take the innermost shell to be of radius  $r_1 = 3L/8$  and width  $r_2 - r_1 = r_1/96$ . We set the mass scales to be such that the Vainshtein scale of the shell  $r_{*M} = r_1/12$  and that of the mass  $r_{*m} = r_1/24$ . Finally, we replace the point mass  $m$  with a constant density sphere of radius  $r_m = r_1/96$ . In Fig. 4, we show the numerical results for the leading order acceleration and first order correction given by Eq. (8) and (9) respectively. Here we plot the acceleration in units of the maximum Newtonian acceleration for a test particle just outside of an infinitesimal shell of radius  $r_1$

$$c_M = \frac{2GM}{3\beta r_1^2}. \quad (34)$$

The numerical calculation of the leading order  $\phi_{\Delta}^{(0)}$  term matches the analytic expression, Eq. (17) to excellent approximation showing the discretization onto the grid does not cause appreciable errors. The first order correction  $\phi_{\Delta}^{(1)}$  becomes comparable to the zeroth order effect when  $r_{*m}/s \sim 1$  implying that the weak-screening approximation applies all the way to separations of a Vainshtein radius of  $m$ . At this point the acceleration, which would be zero in the absence of nonlinearity, becomes a non-negligible fraction of the maximal acceleration  $c_M$ .

Note that for  $M \gg m$ , the validity of the weak-screening approximation extends to separations much smaller than  $r_{*M}$  since nonlinear corrections for  $M$  come in through the characteristic scale of the shell  $r_{*M}/r_1$  rather than the characteristic scale of the separation  $r_{*M}/s$ . Thus in the shell case, the qualitative rule that weak screening applies until the separation becomes comparable to the Vainshtein radius of the individual sources is too conservative if applied to both  $r_{*m}$  and  $r_{*M}$ .

## V. DISCUSSION

The weak-screening regime, where the Vainshtein mechanism is just beginning to suppress fifth forces, exhibits apparent or macroscopic violation of the equivalence principle. We have illustrated this effect through analytic calculations of the acceleration of particles within a mass shell, compensated void, and toward a spherically symmetric mass. Numerical tests show that weak-screening approximation is valid until the bodies are separated by less than a Vainshtein radius.

With an attractive fifth force, massive objects such as dark matter halos in a mass shell or compensated void are attracted to the center of the void with an acceleration proportional to their mass. A cosmological void is also naturally in the weak-screening regime for the cosmologically interesting case where  $H_0 r_c / \beta \sim 1$ . Since the Vainshtein radius of a halo is comparable to its virial radius, the maximal effect will be on halos that are close to a virial radius of the edge. This effect has potential observable consequences for mass segregation near the edge of voids, but it remains to be seen in cosmological simulations whether deviations from the idealizations of spherical symmetry, perfect compensation and constant underdensity mask this effect.

For the infall problem, the two-body interference predicts a reduction of major mass mergers where the bodies are of comparable mass. The infall case also shows how the interference restores Newton's third law or momentum conservation in the joint system.

These effects are signatures of the Vainshtein mechanism, which is itself common to massive gravity, galileon and braneworld scenarios. Our analytic calculations serve as simple illustrations that expose new aspects of the mechanism though constructing realistic cosmological tests of it will require going beyond the idealizations considered here.

## ACKNOWLEDGMENTS

We thank T. Hiramatsu, E. Jennings, K. Koyama, Y. Li, F. Schmidt and E. Babichev for useful conversations. AB was supported in part by ERC project 267117 (DARK) hosted by Universite Pierre et Marie Curie - Paris 6 and acknowledges the hospitality of KICP where part of this work was completed. WH was supported by the KICP through grants NSF PHY-0114422 and NSF PHY-0551142 and an endowment from the Kavli Foundation and its founder Fred Kavli, U.S. Dept. of Energy contract DE-FG02-90ER-40560 and the David and Lucile Packard Foundation. WH acknowledges the hospitality of IAP where part of this work was completed.

- 
- [1] A. Vainshtein, Phys.Lett., **B39**, 393 (1972).
- [2] E. Babichev, C. Deffayet, and R. Ziour, Phys.Rev., **D82**, 104008 (2010), arXiv:1007.4506 [gr-qc].
- [3] H. van Dam and M. Veltman, Nucl.Phys., **B22**, 397 (1970).
- [4] V. Zakharov, JETP Lett., **12**, 312 (1970).
- [5] D. Boulware and S. Deser, Phys.Lett., **B40**, 227 (1972).
- [6] C. de Rham, G. Gabadadze, and A. J. Tolley, Phys.Rev.Lett., **106**, 231101 (2011), arXiv:1011.1232 [hep-th].
- [7] G. Chkareuli and D. Pirtskhalava, Phys.Lett., **B713**, 99 (2012), arXiv:1105.1783 [hep-th].
- [8] K. Koyama, G. Niz, and G. Tasinato, Phys.Rev., **D84**, 064033 (2011), arXiv:1104.2143 [hep-th].
- [9] F. Sbisà, G. Niz, K. Koyama, and G. Tasinato, Phys.Rev., **D86**, 024033 (2012), arXiv:1204.1193 [hep-th].
- [10] A. Nicolis, R. Rattazzi, and E. Trincherini, Phys.Rev., **D79**, 064036 (2009), arXiv:0811.2197 [hep-th].
- [11] C. Deffayet, G. Esposito-Farese, and A. Vikman, Phys.Rev., **D79**, 084003 (2009), arXiv:0901.1314 [hep-th].
- [12] C. Burrage and D. Seery, JCAP, **1008**, 011 (2010), arXiv:1005.1927 [astro-ph.CO].
- [13] N. Kaloper, A. Padilla, and N. Tanahashi, JHEP, **1110**, 148 (2011), arXiv:1106.4827 [hep-th].
- [14] A. De Felice, R. Kase, and S. Tsujikawa, Phys.Rev., **D85**, 044059 (2012), arXiv:1111.5090 [gr-qc].
- [15] R. Kimura, T. Kobayashi, and K. Yamamoto, Phys.Rev., **D85**, 024023 (2012), arXiv:1111.6749 [astro-ph.CO].
- [16] C. de Rham, A. J. Tolley, and D. H. Wesley, (2012), arXiv:1208.0580 [gr-qc].
- [17] C. Deffayet, G. Dvali, G. Gabadadze, and A. I. Vainshtein, Phys.Rev., **D65**, 044026 (2002), arXiv:hep-th/0106001 [hep-th].
- [18] A. Lue and G. Starkman, Phys.Rev., **D67**, 064002 (2003), arXiv:astro-ph/0212083 [astro-ph].
- [19] A. Lue, R. Scoccimarro, and G. D. Starkman, Phys.Rev., **D69**, 124015 (2004), arXiv:astro-ph/0401515 [astro-ph].
- [20] K. Koyama and F. P. Silva, Phys.Rev., **D75**, 084040 (2007), arXiv:hep-th/0702169 [HEP-TH].
- [21] F. Schmidt, Phys.Rev., **D80**, 043001 (2009), arXiv:0905.0858 [astro-ph.CO].
- [22] F. Schmidt, Phys.Rev., **D80**, 123003 (2009), arXiv:0910.0235 [astro-ph.CO].
- [23] F. Schmidt, W. Hu, and M. Lima, Phys.Rev., **D81**, 063005 (2010), arXiv:0911.5178 [astro-ph.CO].
- [24] L. Hui, A. Nicolis, and C. Stubbs, Phys.Rev., **D80**, 104002 (2009), arXiv:0905.2966 [astro-ph.CO].
- [25] W. Hu, Nucl.Phys.Proc.Suppl., **194**, 230 (2009), arXiv:0906.2024 [astro-ph.CO].
- [26] T. Hiramatsu, W. Hu, K. Koyama, and F. Schmidt, (2012), arXiv:1209.3364 [hep-th].
- [27] G. Dvali, G. Gabadadze, and M. Porrati, Phys.Lett., **B485**, 208 (2000), arXiv:hep-th/0005016 [hep-th].
- [28] H. Oyaizu, M. Lima, and W. Hu, Phys.Rev., **D78**, 123524 (2008), arXiv:0807.2462 [astro-ph].
- [29] K. Chan and R. Scoccimarro, Phys.Rev., **D80**, 104005 (2009), arXiv:0906.4548 [astro-ph.CO].
- [30] D.-C. Dai, R. Matsuo, and G. Starkman, Phys.Rev., **D81**, 024041 (2010), arXiv:0811.1565 [astro-ph].